

Article

Recovery of Rare Metals from Superalloy Scraps by an Ultrasonic Leaching Method with a Two-Stage Separation Process

Long Wang^{1,2,3,†}, Sujun Lu^{1,†}, Jiayuan Fan³, Yutian Ma¹, Juan Zhang¹, Shiyang Wang³, Xiaoyao Pei³, Yuan Sun^{3,*}, Guozhi Lv² and Tingan Zhang^{2,*}

¹ State Key Laboratory of Comprehensive Utilization of Nickel and Cobalt Resources, Jinchuan Group Co., Ltd., Jinchang 737100, China; lusujun2022@126.com (S.L.); mayutian666@163.com (Y.M.); zjuan0712@163.com (J.Z.)

² Key Laboratory for Ecological Utilization of Multimetallic Mineral, Ministry of Education, Northeastern University, Shenyang 110819, China; wanglong19880501@163.com (L.W.); lvgz@smm.neu.edu.cn (G.L.)

³ Institute of Metal Research, Chinese Academy of Sciences, Shenyang 110016, China; jyfan@imr.ac.cn (J.F.); sy19880501@126.com (S.W.); xypei@imr.ac.cn (X.P.)

* Correspondence: yuansun@imr.ac.cn (Y.S.); zta2000@163.net (T.Z.); Tel.: +86-13840414962 (Y.S.); +86-13840205331 (T.Z.)

† These authors contributed equally to this work.

Abstract: Superalloy scraps are deemed as potential unconventional sources of rare metals. In this study, an ultrasonic leaching method with a two-stage separation process was proposed. A series of Eh-pH diagrams for rare metals was constructed, and the results indicated that the leaching and separation process could be realized by adjusting the potential and pH values of leaching solutions. In the ultrasonic leaching process, results showed that the economic leaching percentages of Re, Ni, Co, Al, and Cr were 92.3%, 95.2%, 98.5%, 98.7%, and 97.5%, respectively. Compared with conventional leaching, ultrasonic leaching can improve the leaching percentages of rare metals by approximately 20%. In the two-stage separation process, the optimal recovery efficiencies of Al and Cr were 94.6% and 82.1% at a pH of 4.5, and Ni and Co were 99.5% and 98.3% at a pH of 7.5. With a two-stage precipitate process, rare metals can be efficiently recovered without generating any waste acid.

Keywords: superalloy scraps; Eh-pH diagram; ultrasonic leaching; passivation layer; precipitates separation



Citation: Wang, L.; Lu, S.; Fan, J.; Ma, Y.; Zhang, J.; Wang, S.; Pei, X.; Sun, Y.; Lv, G.; Zhang, T. Recovery of Rare Metals from Superalloy Scraps by an Ultrasonic Leaching Method with a Two-Stage Separation Process.

Separations **2022**, *9*, 184. <https://doi.org/10.3390/separations9070184>

Academic Editor: Anastasios Zouboulis

Received: 22 June 2022

Accepted: 19 July 2022

Published: 20 July 2022

Publisher's Note: MDPI stays neutral with regard to jurisdictional claims in published maps and institutional affiliations.



Copyright: © 2022 by the authors. Licensee MDPI, Basel, Switzerland. This article is an open access article distributed under the terms and conditions of the Creative Commons Attribution (CC BY) license (<https://creativecommons.org/licenses/by/4.0/>).

1. Introduction

Due to their excellent high-temperature strength and oxidation resistance, superalloys are widely used in high-temperature structural components of aircraft engines [1]. With the accelerated development of the aerospace industry, the average annual growth rate of superalloys has been more than 20% in recent years. Additionally, with the development of superalloys, the additional scale of rare metals is constantly expanding [2]. For instance, the additional scale of Ni, Co, and Re in second-generation single crystal superalloys has exceeded 70 wt.% [3]. The larger addition scale of rare metals results in a substantial escalation in the price of superalloys [4]. However, such high-value superalloys produce substantial scraps in the production, processing, and service process of superalloys (more than 70% of the total materials) [5]. In addition, considering the extreme scarcity of rare metals resources, superalloy scraps are the crucial unconventional sources of rare metals [6]. The reasonable recovery of rare metals from superalloy scraps can effectively alleviate the problem of insufficient rare metal resources [7].

Due to the excellent corrosion resistance of superalloys, the recycling of superalloys has become quite complicated [8]. Generally, the recycling process can be divided into two processes: pyrometallurgical and hydrometallurgical processes [9]. The pyrometallurgical process is complex and expensive, which contributes to high energy consumption, environmental pollution, even 20% loss of rare metals, and failure to produce pure rare metals from intricate superalloy scraps [10]. While the hydrometallurgical process can be

selective and produce pure rare metals by more environmentally friendly methods with less energy consumption [11], the hydrometallurgical process is a more potent way to recover superalloy scraps [12]. In this process, Al, Cr, W, Ta, and other elements in the superalloy scraps will form a passivation layer on the surface of the superalloy scraps by the extra application of electric field or oxidation [13]. The existence of the passivation layer results in the low leaching efficiency of rare metals from superalloy scraps [14].

To eliminate the influence of the passivation layer in the leaching process, researchers have carried out large numbers of related studies by adjusting the composition of the electrolyte or the type of electric field [15]. The results show that chlorine ion in the electrochemical system has a specific role in promoting the breakdown of the passivation layer on the surface of the superalloy scraps [16]. Chloride ions can penetrate the passivation layer on the surface of the superalloy scraps and combine with metal ions to prevent the formation of the passivation layer in the electrochemical dissolution process [17]. The electrolysis rate of various metals can also be significantly changed by effectively controlling the frequency and amplitude of the alternating current [18]. However, these studies fail to fundamentally eliminate the influence of the passivation layer on the leaching process. Another drawback of the regular process is to deal with quantities of acidic wastewater containing hazardous elements which generate during the leaching and separation process. A large amount of acid was employed to ensure a higher leaching efficiency of rare metals from superalloy, which results in a strong acid still staying in the leaching solution. In the recovery process [19–22], methods such as extraction, ion exchange, liquid membrane separation, and activated carbon adsorption were usually adopted to recycle the rare metals from the leaching solution. These methods were intended to recover rare metals, but left a large amount of waste acid solution, which would cause severe waste acid pollution [23].

Ultrasonic leaching is a potential method to avoid the formation of the passivation layer and facilitate the leaching percentages of rare metals from superalloy scraps [24,25]. Relevant studies showed that due to mechanical agitation by the action of cavitation, the leaching percentages of rare metals from carbonate rock were approximately 20% higher than that of the conventional leaching process [26]. When the ultrasonic leaching process was adopted, the leaching rate of bastnaesite was almost the same as that produced by the conventional leaching process at 85 °C when the leaching temperature was 55 °C [27]. J. Kong et al. showed that ultrasonic leaching could shorten the leaching time under the same leaching percentages [28]. In general, the cavitation can cause the formation of shock waves and micro-jets on the solid surface, which results in more significant impact damage on the solid surface and leads to the efficient breakdown of the passivation layer structure. Cavitation accelerates the diffusion of leaching solution into the solid interior and eventually improves the leaching rate [29,30].

Hence, an ultrasonic leaching process with a two-stage separation process was proposed in this study to improve the leaching percentages of the rare metals from the superalloy scraps and avoid waste acid pollution. Various experimental factors such as ultrasonic power, temperature, time, liquid–solid ratio, and HCl and H₂O₂ dosages were studied. A two-stage separation process was developed to recover rare metals from the leaching solution. The objectives of the paper were to investigate the optimal conditions of the leaching and “two-step” separation procedure to recover rare metals from superalloy scraps, and the ultrasonic leaching mechanism was studied through Scanning electron microscope (SEM) and X ray energy spectrum analysis (EDS).

2. Materials and Methods

2.1. Experimental Materials

In this study, superalloy scraps were obtained from the Institute of Metal Research, the Chinese Academy of Sciences. The contents of Ni, Co, Re, Ta, Cr, and Al in the sample were 62.7, 7.6, 3.1, 6.6, 6.9, and 6.2 wt.%, respectively. Analytical grade reagents such as HCl (mass fraction of 37%), H₂O₂ (volume fraction of 30%), and NaOH were obtained from Shenyang Xinhua Reagent Co., Ltd., Shenyang, China.

2.2. Experimental Method

The schematic diagram of the leaching and separation device was shown in Figure 1. The ultrasonic leaching process was conducted in an ultrasonic bath with an ultrasonic power of 0–600 W (GT1022, Granbo Technology Industrial Shenzhen Co., Ltd., Shenzhen, China). The experimental procedure was as follows: in the leaching process, when the ultrasonic bath was heated to the desired temperature, the sealing beaker containing superalloy scraps and a specific concentration of HCl was placed into the ultrasonic bath. The H₂O₂ was pumped into the flask at a specific rate during the leaching process by a peristaltic pump (BT100S, Baoding Lead Fluid Technology Co., Ltd., Baoding, China). The sealing beaker was taken out from the ultrasonic bath after the leaching process. In the separation process, the pH of the leaching solution was constantly monitored using a pH meter (PHS-25, Shenzhen Yomi Instrument Equipment Co., Ltd., Shenzhen, China). The stirring speed was controlled by a frequency governor with a stirring speed of 100 rpm. When the pH of the leaching solution increased to a specific value, the solutions were separated by a refrigerated centrifuge (DGL-10R, Shandong Boke Biological Industry Co., Ltd., Shandong, China), at 4000 rpm and 15 °C.

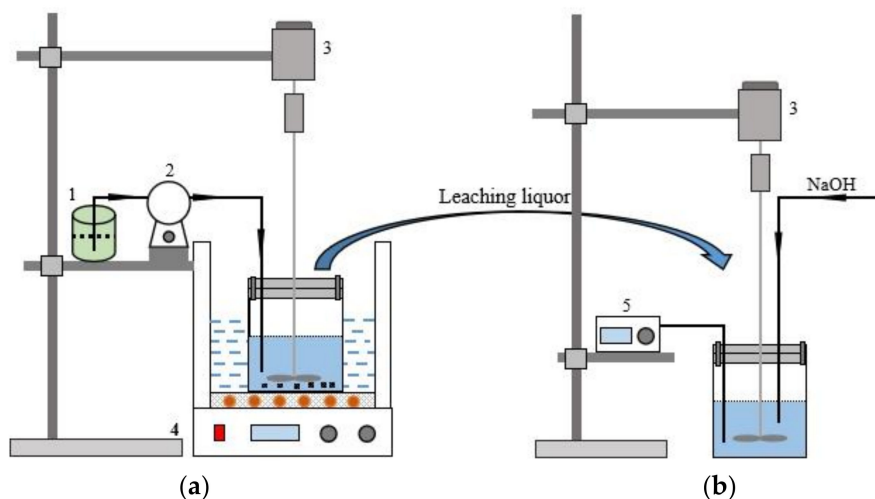


Figure 1. Schematic diagram of the leaching and separation experiment (a) Leaching experimental device; (b) Separation experimental device; (1-H₂O₂; 2-Peristaltic pump; 3-Agitator; 4-Ultrasonic water bath; 5-Potentiometer).

2.3. Analytical Methods

Chemical analysis of the sample was performed using an ICP atomic emission spectrometer (Optima 8300DV, PerkinElmer, Waltham, OR, USA). The leaching percentages were calculated as follows:

$$\eta/\% = m_1 \times 100\%/m_2 \tag{1}$$

where η is the leaching percentages of rare metals from superalloy scraps, %; m_1 is the mass of rare metals in solution, %; and m_2 is the initial mass of superalloy scraps, %.

SEM and EDS (Quanta 450, FEI, Hillsboro, OR, USA) were applied to observe the microscopic morphology of the superalloy scraps and the leaching residues.

3. Results and Discussion

3.1. Eh-pH Diagram of Rare Metals from Superalloy Scrap

In the ultrasonic leaching and separation process, the stable forms of rare metals varied with the different potential and pH values. The Eh-pH diagram can intuitively estimate the potential and pH values of various rare and precious ions for the different stable forms in the leaching solution. For this reason, HSC software (6.0, Outotec, Espoo, Finland) was used to investigate the Eh-pH diagram of rare metals from superalloy scrap to determine

the most favored leaching and separation scheme. The results were shown in Figure 2 and Table 1.

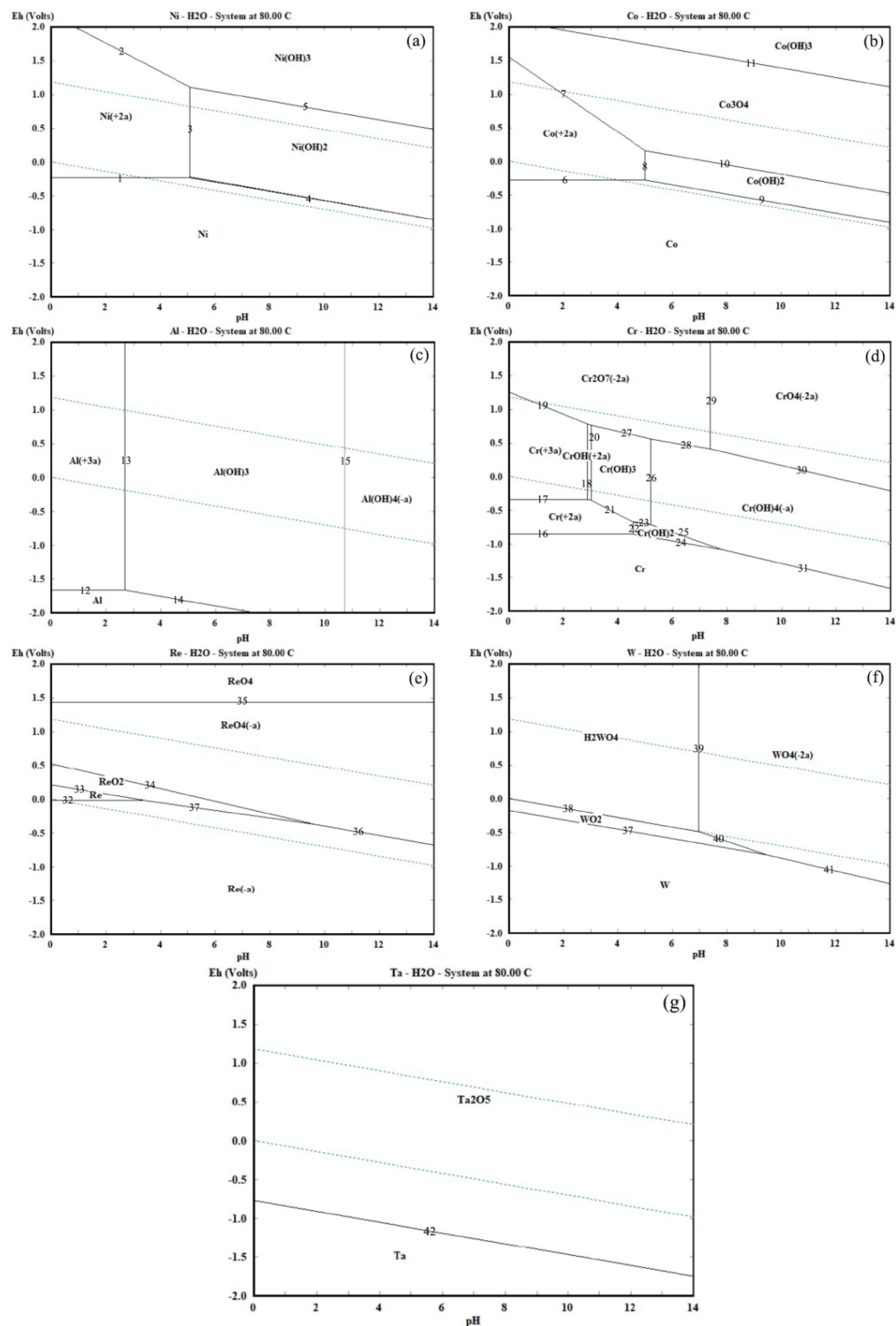


Figure 2. Eh-pH diagram of rare metals in the leaching and separation process at 80 °C. ((a)—Ni; (b)—Co; (c)—Al; (d)—Cr; (e)—Re; (f)—W; and (g)—Ta).

Table 1. The main reactions in the M (Ni, Co, Al, Cr, Re, W, Ta)-H₂O system.

| Elements | No. | Reactions | No. | Reactions |
|----------|-----|---|-----|--|
| Ni | 1 | $Ni^{2+} + 2e = Ni$ | 2 | $Ni^{2+} + 3H_2O = Ni(OH)_3 + 3H^+ + e$ |
| | 3 | $Ni^{2+} + 2H_2O = Ni(OH)_2 + 2H^+$ | 4 | $Ni + 2H_2O = Ni(OH)_2 + 2H^+ + 2e$ |
| | 5 | $Ni(OH)_2 + H_2O = Ni(OH)_3 + H^+ + e$ | | |
| Co | 6 | $Co^{2+} + 2e = Co$ | 7 | $3Co^{2+} + 4H_2O = Co_3O_4 + 8H^+ + 2e$ |
| | 8 | $Co^{2+} + 2H_2O = Co(OH)_2 + 2H^+$ | 9 | $Co + 2H_2O = Co(OH)_2 + 2H^+ + 2e$ |
| | 10 | $3Co(OH)_2 + H_2O = Co_3O_4 + 8H^+ + 8e$ | 11 | $Co_3O_4 + 5H_2O = 3Co(OH)_3 + H^+ + e$ |
| Al | 12 | $Al^{3+} + 3e = Al$ | 13 | $Al^{3+} + 3H_2O = Al(OH)_3 + 3H^+$ |
| | 14 | $Al + 3H_2O = Al(OH)_3 + 3H^+ + 3e$ | 15 | $Al(OH)_3 + H_2O = Al(OH)_4^- + H^+$ |
| Cr | 16 | $Cr^{2+} + 2e = Cr$ | 17 | $Cr^{3+} + e = Cr^{2+}$ |
| | 18 | $Cr^{3+} + H_2O = CrOH^{2+} + H^+$ | 19 | $2Cr^{3+} + 7H_2O = Cr_2O_7^{2-} + 14H^+ + 6e$ |
| | 20 | $CrOH^{2+} + 2H_2O = Cr(OH)_3 + 2H^+$ | 21 | $Cr^{2+} + 3H_2O = Cr(OH)_3 + 3H^+ + e$ |
| | 22 | $Cr^{2+} + 2H_2O = Cr(OH)_2 + 2H^+$ | 23 | $Cr(OH)_2 + H_2O = Cr(OH)_3 + H^+ + e$ |
| | 24 | $Cr + 2H_2O = Cr(OH)_2 + 2H^+ + 2e$ | 25 | $Cr(OH)_2 + 2H_2O = Cr(OH)_4^- + 2H^+ + e$ |
| | 26 | $Cr(OH)_3 + H_2O = Cr(OH)_4^- + H^+$ | 27 | $2Cr(OH)_3 + H_2O = Cr_2O_7^{2-} + 8H^+ + 6e$ |
| | 28 | $2Cr(OH)_4^- = Cr_2O_7^{2-} + H_2O + 6H^+ + 6e$ | 29 | $Cr_2O_7^{2-} + H_2O = 2CrO_4^{2-} + 2H^+$ |
| | 30 | $Cr(OH)_4^- = CrO_4^{2-} + 4H^+ + 3e$ | 31 | $Cr + 4H_2O = Cr(OH)_4^- + 4H^+ + 3e$ |
| Re | 32 | $Re + e = Re^-$ | 33 | $Re^- + 2H_2O = ReO_2 + 4H^+ + 5e$ |
| | 34 | $ReO_2 + 2H_2O = ReO_4^- + 4H^+ + 3e$ | 35 | $ReO_4 + e = ReO_4^-$ |
| | 36 | $Re^- + 4H_2O = ReO_4^- + 8H^+ + 8e$ | 37 | $Re^- + 2H_2O = ReO_2 + 4H^+ + 5e$ |
| W | 37 | $W + 2H_2O = WO_2 + 4H^+ + 4e$ | 38 | $WO_2 + 2H_2O = H_2WOH_4 + 2H^+ + 2e$ |
| | 39 | $WO_4^{2-} + 2H^+ = H_2WOH_4$ | 40 | $WO_2 + 2H_2O = WO_4^{2-} + 4H^+ + 2e$ |
| | 41 | $W + 4H_2O = WO_4^{2-} + 8H^+ + 6e$ | | |
| Ta | 42 | $2Ta + 5H_2O = Ta_2O_5 + 10H^+ + 10e$ | | |

Figure 2a shows the Eh-pH diagram for the Ni-H₂O system at 80 °C. It is observed that at low potentials and in the whole pH range, Ni is stable as a species. When the pH value is lower than 5.2 and the potential value is higher than -0.22 V, Ni primarily exists as Ni²⁺ in the Ni-H₂O system. When the pH value is higher than 5.2, Ni primarily exists as Ni(OH)₂ and Ni(OH)₃ in the Ni-H₂O system. For Co, in Figure 2b, it is observed that when the potential value is lower than -0.82 V at the whole pH range, Co is stable as a species. Figure 2b also shows that the stability regions of Co²⁺ include a region (-0.25–1.55 V at pH 0–5.2). When the pH value is higher than 5.2, Co primarily exists as Co(OH)₂ at a very narrow region (-0.82–0.25 V at pH 5.2–14). Hence, the optimal pH value for leaching of Ni and Co from superalloy scraps should be 0–5.2 at the potential value of -0.25–1.52 V, and the optimal pH value for the separation process of Ni and Co from leaching liquid should be 5.2–14.

In Figure 2c, when the pH value is lower than 2.83 and the potential value is higher than -1.72 V, Al primarily exists as Al³⁺ in the Al-H₂O system. At the pH value between 2.8 and 10.8, Al primarily exists as Al(OH)₃ in the Al-H₂O system. While Al(OH)₄⁻ is the predominant stable species in the Al-H₂O system when the pH value is high than 10.8. For Cr, when the pH value is lower than 2.9 at the potential value between -0.36 and 1.42 V, Cr³⁺ is the major leaching product. At the pH value between 3.1 and 5.2 and the potential value between -0.36 and 0.62 V, Cr(OH)₃ is the main stable species. The formation of this aluminum and chromium oxide has been demonstrated to be the composition of a passivation layer on the superalloy scrap surface in leaching solutions [15], which will lead to the passivation phenomenon on the superalloy scrap surface during the leaching process. To avoid the formation of aluminum and chromium oxide, it is extremely important to adjust the potential and pH value of leaching solutions during the leaching process of superalloy scraps. Hence, the optimal potential values for leaching of Al and Cr from superalloy scrap should be -0.36 and 1.42 V at the pH value of 0–2.9, and the optimal

pH value for the separation process of Al and Cr as mixed hydroxide precipitates from leaching solution should be maintained between 3.1 and 5.2.

The Eh-pH diagram of the Re-H₂O system at 80 °C is given in Figure 2e. The pH and potential values play an important role in determining which species are produced during the leaching process of Re. It is observed that the stability region of ReO₄⁻ is located in the area with the potential value of 0.52–1.43 V at the whole pH range, which is a wide area in the thermodynamic stability region of water. At a high potential value (1.43–2.0 V), Re primarily exists as ReO₄ in the Re-H₂O system. When the pH of the Re-H₂O system is relatively low (0–3.3), Re exists within the region of 0 to 0.23 V. ReO₂ exists in a very narrow region of (–0.25–0.52 V at pH 0–9.5). The formation of Re⁻, Re, ReO₂, and ReO₄ hurt the leaching progress of Re from superalloy scrap. Therefore, the optimal potential value for leaching and separation of Re from superalloy scrap should be 0.52–1.43 V.

Figure 2f shows the Eh-pH diagram of the W-H₂O system at 80 °C. It is observed that the stability region of W is located in the area when the potential value is lower than –1.25 V at the whole pH range. When the potential value of the leaching solution is a relatively narrow distribution (–0.76–0 V), the WO₂ exists within the pH range of 0 to 9.2. At a high potential value of 0 to 2.12 V, H₂WO₄ exists within the pH range of 0–7.0, and WO₄²⁻ stably exists at the pH value above 7.0 in the thermodynamic stability region of water. As for Ta, Figure 2g indicated Ta can exhibit two different phases like Ta and Ta₂O₅. As the pH value increases from 0 to 14, the formation potential of Ta₂O₅ decreases from –0.75 to –1.71 V. The formation of WO₃ and Ta₂O₅ has been demonstrated to be the composition of the product layer on the superalloy scrap surface in leaching solutions [15], which may obstacle to the dissolving of the superalloy scraps during the leaching process. To avoid the formation of the product layer, it is extremely important to adjust the potential and pH value of leaching solutions during the leaching process of superalloy scrap.

In conclusion, there are a series of stable thermodynamic regions of various rare metal ions under different potential and pH value conditions. The optimal potential values range for leaching of rare metals from superalloy scraps should be 0.52 to 1.43 V at the pH value of 0 to 2.8. For the separation process, the optimal pH values range for Ni and Co should be maintained between 5.2 and 14, and the optimal pH values range for Al and Cr should be maintained between 3.1 and 5.2. Additionally, Re will remain in the solution in the form of ReO₄⁻. W and Ta will stay in the leaching residues in the form of WO₃ and Ta₂O₅.

3.2. Ultrasonic Leaching Process of Rare Metals from Superalloy Scraps

3.2.1. Effect of Ultrasonic Power

The leaching percentages of rare metals at different ultrasonic powers are presented in Figure 3.

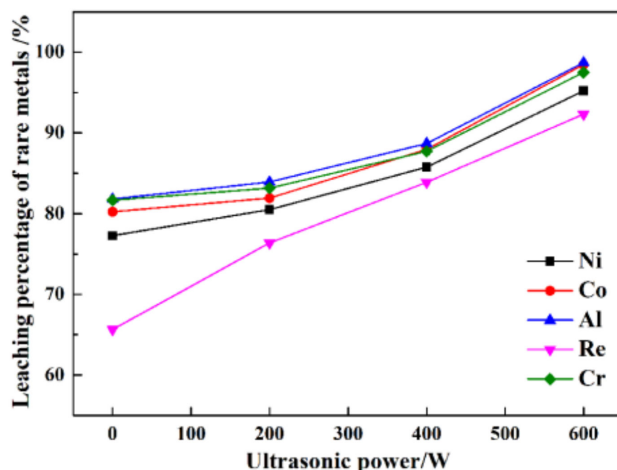


Figure 3. The leaching percentages of rare metals under different ultrasonic powers.

In Figure 3, at 60 min with ultrasonic power of 0 W, the leaching percentages of Re, Ni, Co, Al, and Cr are only 65.6%, 77.3%, 80.2%, 81.8%, and 81.6%, respectively. Within 60 min at 200 W of ultrasonic power, the leaching percentages of Re, Ni, Co, Al, and Cr are only 76.4%, 80.5%, 81.9%, 83.9%, and 83.2%, respectively. While at 600 W, the leaching percentages of Re, Ni, Co, Al, and Cr are 92.3%, 95.2%, 98.5%, 98.7%, and 97.5%, respectively. The results indicate that ultrasonic leaching can improve the leaching percentages of Ni, Co, Al, and Cr by approximately 20%, especially, for Re, the leaching percentages can be improved by 40%. The leaching percentages of Re, Ni, Co, Al, and Cr under high ultrasonic power are much higher than that under using low ultrasonic power. The results show that ultrasonic power can dramatically affect the leaching percentages of rare metals from superalloy scraps.

3.2.2. Effect of Temperature

The leaching percentages of rare metals under various temperatures are presented in Figure 4.

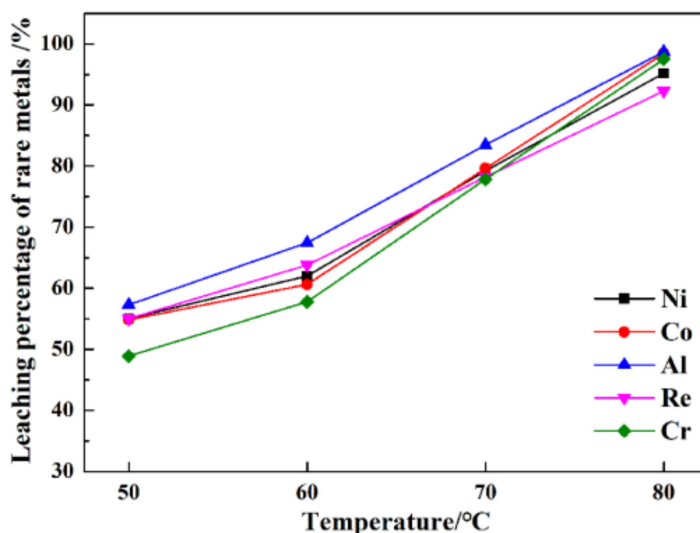


Figure 4. The leaching percentages of rare metals under various temperatures.

From Figure 4, at 50 °C, the leaching percentages of Re, Ni, Co, Al, and Cr are only 55.1%, 55.1%, 54.8%, 57.3%, and 48.9%, respectively. In contrast, much higher efficiency is obtained from the ultrasonic leaching process at 80 °C, i.e., 92.3%, 95.2%, 95.4%, 98.1%, and 98.5%, respectively. The leaching temperature is conducive to increasing the leaching percentages of rare metals from superalloy scraps. Compared with conventional leaching, the leaching percentages of rare metals from superalloy scraps are much higher than those from conventional leaching. An increase in the leaching temperature is conducive to ultrasonic cavitation.

3.2.3. Effect of Time

The leaching percentages of rare metals at various times are presented in Figure 5.

As shown in Figure 5, with increasing time, the leaching percentages of Re, Ni, Co, Al, and Cr increase linearly. When the time is extended from 30 min to 120 min, the leaching percentages of Re, Ni, Co, Al, and Cr increase from 61.2%, 67.5%, 66.6%, 78.3%, and 65.8% to 99.1%, 95.7%, 99.9%, 99.9%, and 99.8%, respectively. At 60 min, the leaching percentages of Re, Ni, Co, Al, and Cr are 92.3%, 95.2%, 98.5%, 98.7%, and 97.5%, respectively. With the continuation of the ultrasonic leaching process (>60 min), the leaching percentages of Re, Ni, Co, Al, and Cr are not further elevated. After a leaching time of 120 min, the leaching percentages of Re, Ni, Co, Al, and Cr are only 6.8%, 0.5%, 1.4%, 1.2%, and 2.3% higher than those obtained after a leaching time of 60 min.

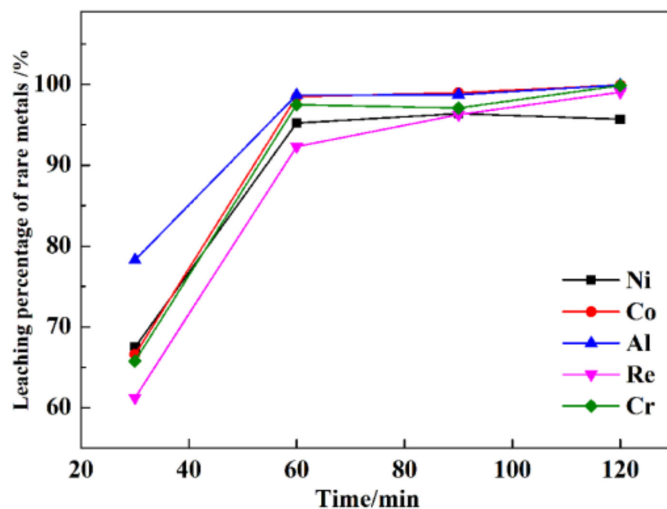


Figure 5. The leaching percentages of rare metals under various times.

3.2.4. Effect of Liquid-Solid Ratio

The leaching percentages of rare metals at different liquid–solid ratios are presented in Figure 6.

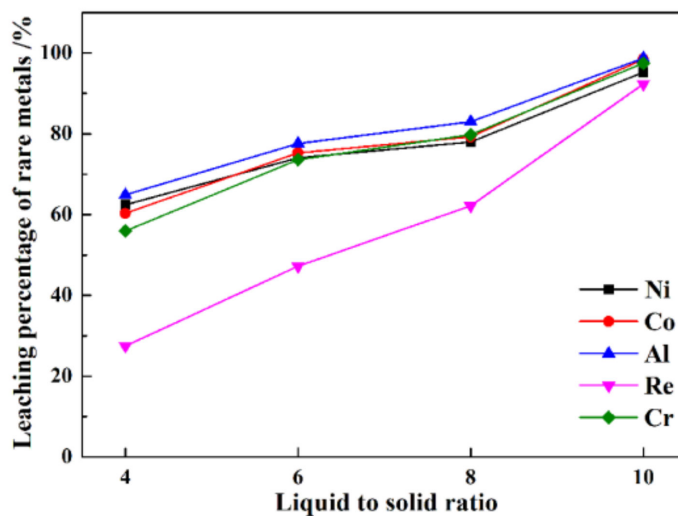


Figure 6. The leaching percentages of rare metals under various liquid–solid ratios.

From Figure 6, at a liquid–solid ratio of 4, the leaching percentages of Re, Ni, Co, Al, and Cr are only 27.5%, 62.5%, 60.3%, 64.9%, and 55.9%, respectively. At a higher liquid–solid ratio of 10, a much higher efficiency is obtained, i.e., 92.3%, 95.2%, 95.4%, 98.1%, and 98.5%, respectively. The results show that a higher leaching liquid–solid ratio results in higher leaching percentages of rare metals from superalloy scraps. Nonetheless, a higher liquid–solid ratio results in a larger dose of leaching reagents when treated with the same mass of superalloy scraps. Therefore, a compromise must be made between the maximum tolerable amount of reagent and the leaching percentages of rare metals from superalloy scraps.

3.2.5. Effect of HCl and H₂O₂ Dosages

Figure 7 shows the leaching percentages of rare metals under various HCl and H₂O₂ dosages.

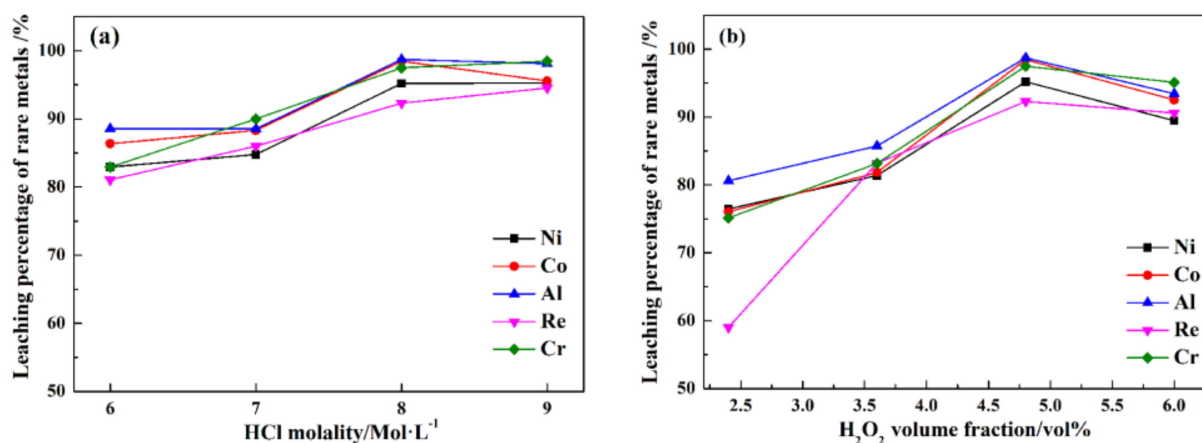


Figure 7. The leaching percentages of rare metals in different HCl (a) and H₂O₂ dosages (b).

In Figure 7a, HCl can enhance the ultrasonic leaching process of rare metals recovery from superalloy scraps. When the HCl molality increases from 6 to 8 mol/L, the leaching percentages of Re, Ni, Co, Al, and Cr increase from 81.1%, 82.9%, 86.4%, 88.5%, and 82.9% to 92.3%, 95.2%, 98.5%, 98.7%, and 97.5%, respectively. As the HCl molality increases to 9 Mol/L, the leaching percentages of Re, Ni, Co, Al, and Cr are 94.5%, 95.2%, 95.4%, 98.1%, and 98.5%, respectively, and the improvement effect is not obvious. In Figure 7b, when the H₂O₂ dose increases from 2.4 to 4.8 vol%, the leaching percentages of Re, Ni, Co, Al, and Cr increase from 58.9%, 76.5%, 76.1%, 80.6%, 75.1%, and 25.7% to 92.3%, 95.2%, 98.5%, 98.7%, and 97.5%, respectively. Increasing the H₂O₂ dose can effectively improve the leaching percentages of Ni, Co, Al, and Cr, especially the leaching rate of Re. As the H₂O₂ dose increases to 6.0 vol%, the leaching percentages of Re, Ni, Co, Al, and Cr are 90.6%, 89.4%, 92.5%, 93.4%, and 95.1%, respectively. It is observed that the improvement in the leaching percentages of Re, Ni, Co, Al, and Cr are not obvious as the dose of H₂O₂ continues to improve.

3.2.6. Leaching Mechanism of Superalloy Scraps in Different Leaching Processes

To elucidate the mechanism by which rare metals are leached from superalloy scraps in different leaching processes, SEM and EDS analyses of superalloy scraps and the leaching residues in different leaching processes were conducted, and the results are shown in Figure 8.

From Figure 8a, the morphology of superalloy scraps presents a smooth surface with some particles attached to the surfaces. The EDS results show that region A consists of Ni, O, Al, Co, Cr, Mo, W, Ta, and Re. In Figure 8b, in the conventional leaching process (0 W of ultrasonic power), at a leaching time of 60 min, the surface of the leaching residues is smooth with obvious cracks and particles attached. The EDS analysis results of region B show that the surface of the leaching residues is mainly composed of O, Al, Cl, Cr, Ni, Co, Mo, Ta, W, Re, etc. Compared with the original composition (Figure 8a), there is a conspicuous enrichment of Cr, Ta, W, and O. In the conventional leaching process, a passivation layer, consisting of Ta, W, Cr, and O, is formed on the surface of the superalloy and ultimately reduces the leaching percentages of rare metals from superalloy scraps. In Figure 8c, at a leaching time of 60 min and an ultrasonic power of 600 W, the leaching residues mainly exist in granular structures and the original organization of the superalloy scrap has completely disappeared. The EDS analysis results of region C show that the leaching residues are primarily composed of O, Ta, and W. In the ultrasonic leaching process, after a leaching time of 60 min, elements such as Al, Ni, Co, Mo, and Re in the superalloy scraps have been entirely dissolved into the leaching solution, while W and Ta have formed Ta₂O₅ and WO₃ and remained in the leaching residues.

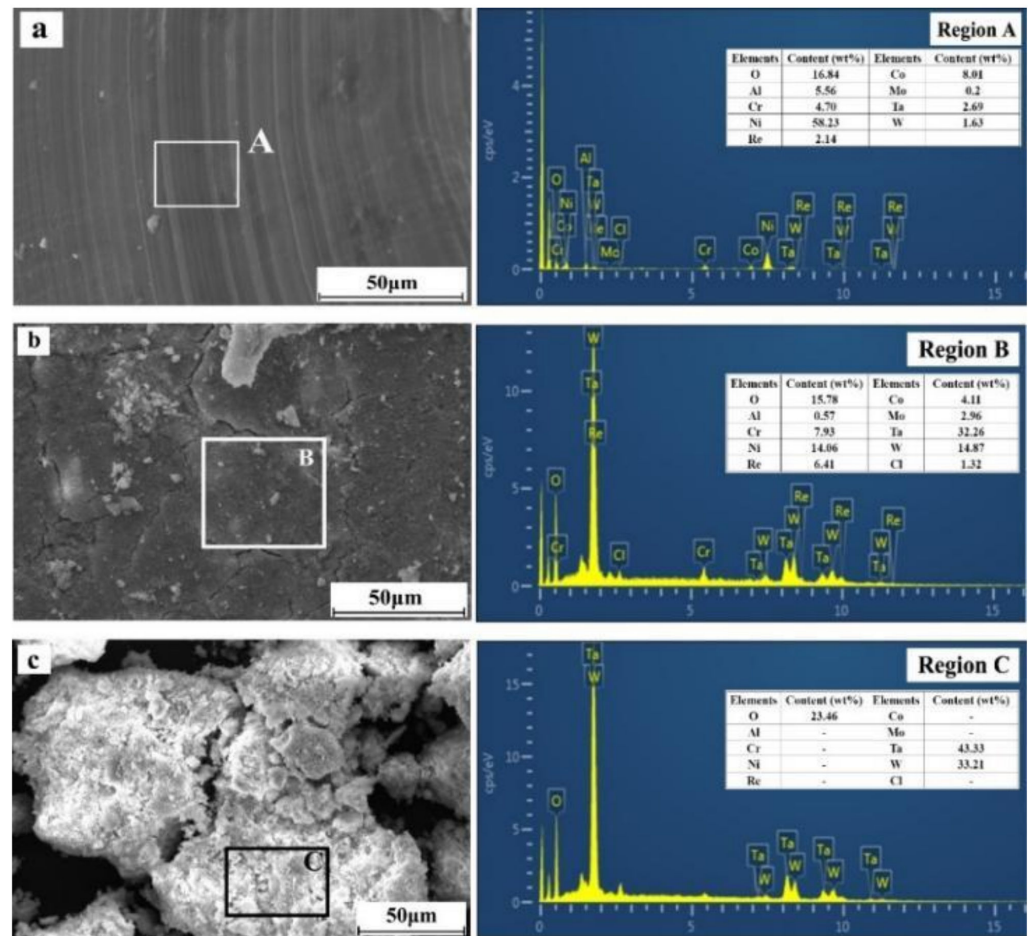


Figure 8. SEM and EDS analyses of the superalloy scraps and leaching residues ((a)—superalloy scraps; (b)—conventional leaching residues; (c)—ultrasonic leaching residues).

In fact, in the conventional leaching process, the existence of the passivation layer reduces the reaction interface between the superalloy scraps and the leaching solution, leading to a decrease in the leaching percentages of rare metals from superalloys. In the ultrasonic leaching process, a large number of cavitation bubbles can be formed at the liquid–solid contact interface due to the action of ultrasonic cavitation. By breaking the cavitation bubbles, a large number of microjets can be generated and continuously impact the surface of the superalloy. The cavitation can avoid the formation of the passivation layer and improves the leaching percentages of rare metals from superalloy scraps.

3.3. Gradient Precipitate Separation of Rare Metals from the Leaching Solution

3.3.1. Precipitate Separation of Rare Metals from the Leaching Solution

To elucidate the rule of rare metals ion distribution in both the liquid and solid phases, the separation process was conducted by the sequential addition of NaOH solution with a molality of 2 mol/L. Figure 9 presents the content of rare metal ions in the solution at different pH values.

From Figure 9, at pH values of 0.5 to 4.5, due to the dilution effect of the NaOH solution, the contents of Ni²⁺ and Co²⁺ decrease slowly. At the pH value exceeds 7.5, the concentrations of Ni²⁺ and Co²⁺ in the leaching solution no longer change, which indicates that Ni²⁺ and Co²⁺ have been completely precipitated. For Al and Cr, with a pH value range of 0.5 to 4.5, Al³⁺ and Cr³⁺ in the solution form an Al/Cr mixed hydroxide precipitate, resulting in a rapid reduction in the concentration of Al³⁺ and Cr³⁺ in the solution. When the pH value increases to 10, the Al/Cr mixed hydroxide precipitate can be selectively

redissolved in the NaOH solution, leading to the accumulation of Al^{3+} and Cr^{3+} in the leaching solution. Re can exist in the leaching solution in the form of ReO_4^- and cannot react with NaOH. The decreasing concentration of Re is due to attenuation by the addition of NaOH solution and the precipitate separation loss of the mixed hydroxide precipitate. The precipitate separation loss can be recovered in the filtrate by the filtration process of the separation.

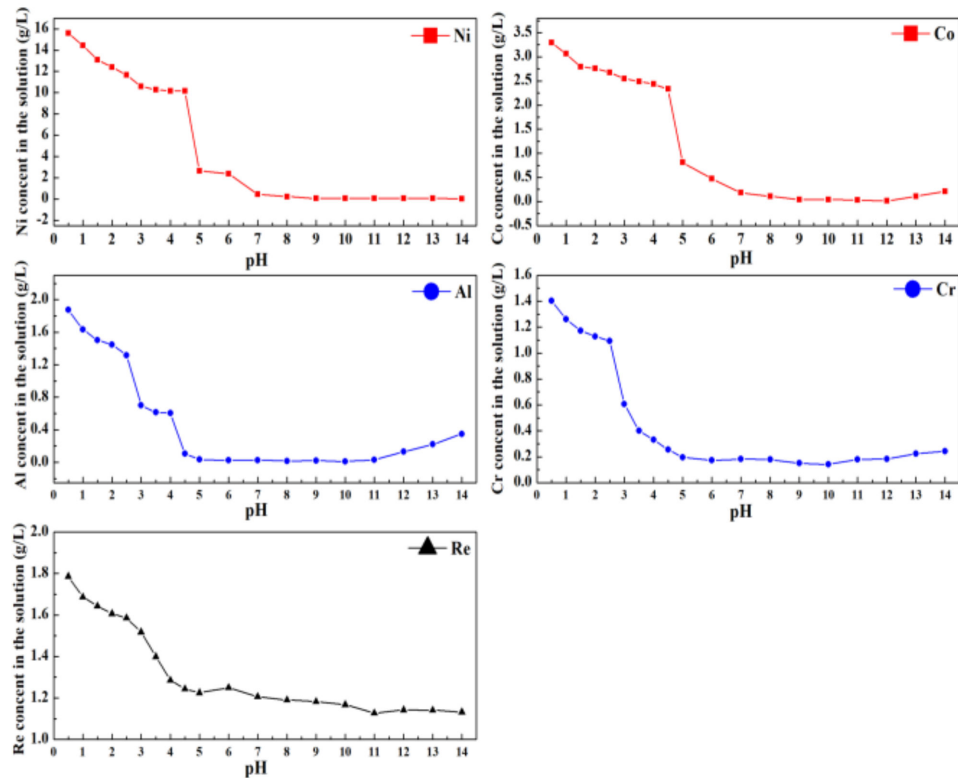


Figure 9. The content of rare metals ions in leaching solution at different pH values.

3.3.2. Two-Stage Precipitates Separation of Rare Metals from the Leaching Solution

Based on the rule of rare metals ion distribution in both liquid and solid phases, the two-stage separation process was conducted at pH values of 4.5 and 7.5. The chemical content of the leaching solution at different pH values is presented in Table 2.

Table 2. Chemical content of the leaching solution at different pH values (g/L).

| pH | Elements | | | | |
|-----|----------|------|------|------|------|
| | Ni | Co | Al | Cr | Re |
| 0.5 | 15.59 | 3.29 | 1.87 | 1.40 | 1.78 |
| 4.5 | 9.74 | 2.12 | 0.10 | 0.25 | 1.24 |
| 7.5 | 0.05 | 0.04 | 0.01 | 0.15 | 1.18 |

In the first stage, by controlling the pH of the solution at 4.5, the predominant Al^{3+} and Cr^{3+} contents in the solution are removed as Al/Cr mixed hydroxide precipitates (MHPs). At a pH value of 4.5, Table 2 shows that the concentrations of Al and Cr were 0.10 and 0.25 g/L, respectively, and approximately 94.6% of Al and 82.1% of Cr in the leaching solution were removed by filtering the solid from the solution with minimal loss of Ni and Co. The lost part of Ni and Co can be recycled by redissolving the Al and Cr mixed hydroxide precipitate into the NaOH solution. In addition, the Al and Cr-containing solution could be reused as raw materials to recover Al and Cr.

In the second stage, at a pH value of 7.5, the contents of Ni, Co, Al, Cr, and Re in the leaching solution are 0.05, 0.04, 0.01, 0.15, and 1.18 g/L, respectively. Nearly 99.5% of Ni and 98.3% of Co in the solution has been removed as Ni/Co mixed hydroxide precipitates (MHPs), which are the most important ternary battery material precipitates with a high commercial utilization value. In the case of ReO_4^- rich solutions, due to the different solubilities of the Re and other compounds, the Re compound can be crystallized, purified, and used as a raw material for rhenium-containing products. The remaining liquid, which still contains a certain amount of alkali, can be recycled in the first stage of the separation of rare metals from superalloy scraps.

3.3.3. Morphology Analysis of Two-Stage Precipitates Separation Products

The SEM and EDS analyses were conducted on products with different pH values, as shown in Figure 10.

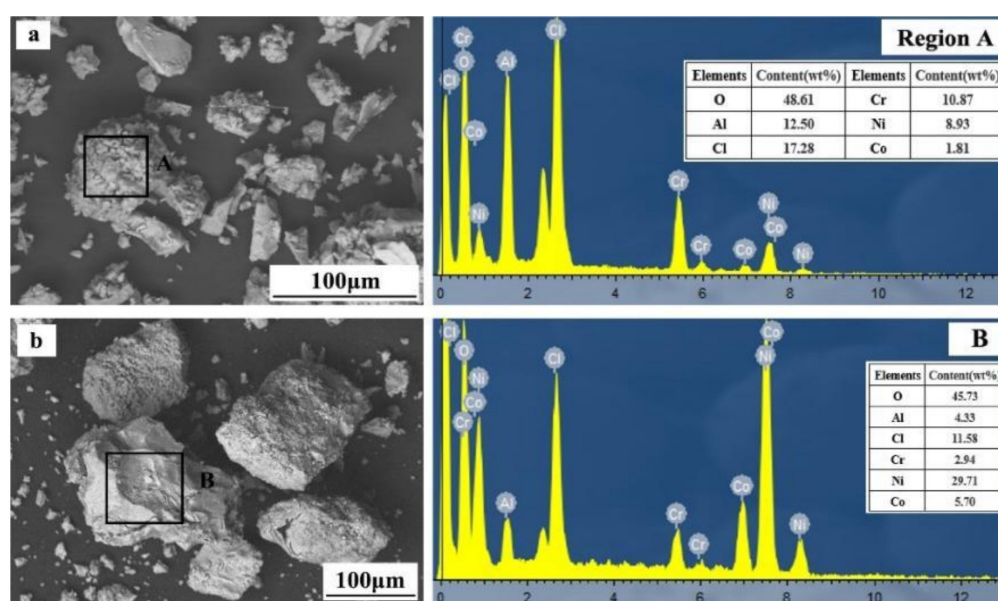


Figure 10. SEM and EDS analyses of products with different pH values ((a)—pH of 4; (b)—pH of 7.5).

From Figure 10a, at a pH value of 4.5, the separation products are mostly particle structures with significant differences in particle size and shape. EDS analysis results show that region A mainly consists of Al, Cr, Ni, Co, and O. As shown in Figure 10b, at a pH value of 7.5, the precipitated product has a particle structure. Compared with the separation products at a pH value of 4.5, the particles are more conventional and larger. With the increase of pH value, the separation crystallization in the leaching solution becomes much more complete. The EDS analysis results show that region B mainly consists of Al, Cr, Ni, Co, and O. The minuscule contents of Al and Cr in the precipitated product indicate that the majority of Al and Cr were separated from the solution in the first stage.

In general, by a two-stage precipitates separation process of rare metals from the leaching solution, the designated pH values in the solution result in most of the component metals separating from the leaching solution while leaving only a Re-rich solution, without waste acid or alkali pollution.

4. Conclusions

In this study, an ultrasonic leaching method with a two-stage separation process for recovering rare metals from superalloy scraps was investigated. The corresponding conclusions are as follows:

(1) The analysis results of Eh-pH diagrams indicated that the leaching and separation process of rare metals from superalloy scraps can be realized by adjusting the potential and pH values of leaching solutions.

(2) The economic leaching percentages of Re, Ni, Co, Al, and Cr were 92.3%, 95.2%, 98.5%, 98.7%, and 97.5%, respectively, under the conditions as ultrasonic power of 600 W, temperature of 80 °C, leaching time of 60 min, liquid–solid ratio of 10, HCl molality of 8 Mol/L and H₂O₂ volume fraction of 4.8 vol%.

(3) The increase in the leaching percentages of rare metals from superalloy scraps can be attributed to ultrasonic cavitation, which was credited with preventing the formation of the passivation layer and enhancing the leaching process.

(4) At a pH value of 4.5, approximately 94.6% of Al and 82.1% of Cr in the leaching solution will be removed as Al/Cr mixed hydroxide precipitate. At a pH of 7.5, nearly 99.5% of Ni and 98.3% of Co in the solution will be removed as Ni/Co mixed hydroxide precipitates, leaving a Re-rich solution for further purification and production.

In this paper, the leaching percentages of rare metals from superalloy scraps can be enhanced by ultrasonic cavitation. The two-stage gradient separation process can significantly improve the recovery efficiency of superalloy scraps from leaching solutions without waste acid or alkali pollution.

Author Contributions: Methodology, S.W. and T.Z.; validation, S.W.; formal analysis, Y.M.; investigation, L.W., S.L., J.F., J.Z., S.W., X.P., Y.S., G.L. and T.Z.; resources, Y.S., G.L. and T.Z.; data curation, X.P.; writing—original draft preparation, L.W., S.L. and J.F.; writing—review and editing, L.W.; visualization, S.L.; supervision, G.L.; project administration, X.P.; funding acquisition, L.W., Y.M., Y.S. and T.Z. All authors have read and agreed to the published version of the manuscript.

Funding: This research was funded by State Key Laboratory of Comprehensive Utilization of Nickel and Cobalt Resources (E041A104Z1), Chinese Academy of Sciences (E055A101), Science and technology project of Shen-Fu Reform and innovation Demonstration Zone (2021JH15), Shenyang Science and Technology Plan (20-203-5-19), National Natural Science Foundation of China (U1710257), and National Key Research and Development Program of China (2021YFB3700401).

Conflicts of Interest: The authors declare no conflict of interest.

References

1. Xu, H.; Zhang, Y.H.; Fu, H.D.; Xue, F.; Zhou, X.Z.; Xie, J.X. Effects of boron or carbon on solidification behavior of Co-Ni-Al-W-based superalloys. *J. Alloys Compd.* **2022**, *891*, 161965. [[CrossRef](#)]
2. Liu, J.D.; Li, B.; Sun, Y.; Jin, T.; Sun, X.F.; Hu, Z.Q. Transient liquid-phase bonding of superalloy K465 using a Ni–Cr–Fe–B–Si amorphous interlayer alloy. *Rare Met.* **2020**, *9*, 3408–3412. [[CrossRef](#)]
3. Liu, E.; Guan, X.; Zheng, Z. Effect of rhenium on solidification and segregation of nickel-based superalloy. *Rare Met.* **2011**, *30*, 320–322. [[CrossRef](#)]
4. Lu, X.; Tian, S.; Yu, X.; Wang, C.X. Oxidation behavior of a single-crystal Ni-base superalloy in the air at 900 and 1050 °C. *Rare Met.* **2011**, *30*, 439–442. [[CrossRef](#)]
5. Chen, Z.H.; Chen, Z.B.; Sun, Y.; Tang, J.J.; Hou, G.C.; Zhang, H.Y.; Liu, W.Q. Research progress and future development direction of recycling and reuse of superalloy scraps. *Mater. Rev.* **2019**, *33*, 3654–3661. (In Chinese)
6. Kim, M.S.; Lee, J.C.; Park, H.S.; Jun, M.J. A multistep leaching of nickel-based superalloy scraps for selective dissolution of its constituent metals in hydrochloric acid solutions. *Hydrometallurgy* **2018**, *176*, 235–242. [[CrossRef](#)]
7. Sunder, G.; Adhikari, S.; Rohanifar, A.; Kirchhoff, J.R. Evolution of environmentally friendly strategies for metal extraction. *Separations* **2020**, *7*, 4. [[CrossRef](#)]
8. Debarbadillo, J.J. Nickel-base superalloys, physical metallurgy of recycling. *Metall. Trans. A* **1983**, *14*, 329–341. [[CrossRef](#)]
9. Tian, Q.H.; Gan, X.D.; Yu, D.W.; Cui, F.H.; Guo, X.Y. One-step and selective extraction of nickel from nickel-based superalloy by molten zinc. *Trans. Nonferrous Met. Soc. China* **2021**, *31*, 1828–1841. [[CrossRef](#)]
10. Cui, F.H.; Wang, G.; Yu, D.W.; Gan, X.D.; Tian, Q.H.; Guo, X.Y. Towards “zero waste” extraction of nickel from scrap nickel-based superalloy using magnesium. *J. Clean. Prod.* **2020**, *262*, 121275. [[CrossRef](#)]
11. Srivastava, R.R.; Kim, M.S.; Lee, J.C.; Jha, M.K.; Kin, B.S. Resource recycling of superalloys and hydrometallurgical challenges. *J. Mater. Sci.* **2014**, *49*, 4671–4686. [[CrossRef](#)]
12. Srivastava, R.R.; Kim, M.S.; Lee, J.C. A novel aqueous processing of the reverted turbine-blade superalloy for rhenium recovery. *Ind. Eng. Chem. Res.* **2016**, *55*, 8191–8199. [[CrossRef](#)]

13. Olbrich, A.; Meece-marktscheffek, J.; Jahn, M.; Zertani, R.; Stoller, V.; Erb, M.; Heine, K.H.; Kutzler, U. Recycling of Superalloys with the Aid of an Alkali Metal Salt Bath. U.S. Patent 20090255372A1, 15 October 2009.
14. Guevel, Y.; Gregoire, B.; Cristobal, M.J.; Feaugas, X.A.; Oudriss, A.; Pedraza, F. Dissolution and passivation of aluminide coatings on the model and Ni-based superalloy. *Surf. Coat. Technol.* **2019**, *357*, 1037–1047. [[CrossRef](#)]
15. Wang, L.; Wang, S.Y.; Song, Z.Y.; Sun, Y.; Zhou, Y.Z.; Pei, X.P.; Zhang, H.Y. Electrochemical dissolution behaviors of scrap superalloys in different electrolytes. *JOM* **2021**, *73*, 1978–1986. [[CrossRef](#)]
16. Simchen, F.N.; Masoud-Nia, N.; Mehner, T.; Lampke, T. Corrigendum. formation of corundum-rich alumina coatings on low-carbon steel by plasma electrolytic oxidation. *IOP Conf. Ser. Mater. Sci. Eng.* **2021**, *651*, 32039–32045.
17. Feng, R.S.; Xu, S.M.; Liu, J.; Wang, C.Y. The influence of Cl on the electrochemical dissolution of cobalt white alloy containing high silicon in a sulfuric acid solution. *Hydrometallurgy* **2014**, *142*, 12–22. [[CrossRef](#)]
18. Palant, A.A.; Levchuk, O.M.; Bryukvin, V.A.; Levin, A.M. Complex electrochemical processing of the metallic wastes from a rhenium-containing nickel superalloy in the sulfuric acid electrolyte. *Russ. Metall.* **2011**, *6*, 589–593. [[CrossRef](#)]
19. Soledad, C.; Rafael, L. Recent advances in extraction and stirring integrated techniques. *Separations* **2017**, *4*, 6.
20. Ueda, Y.; Morisada, S.; Kawakita, H.; Ohto, K. Selective Extraction of platinum(IV) from the simulated secondary resources using simple secondary amide and urea extractants. *Separations* **2021**, *8*, 139. [[CrossRef](#)]
21. Torrecartas, S.; Meseguerrlloret, S. Recent advances in molecularly imprinted membranes for sample treatment and separation. *Separations* **2020**, *7*, 69. [[CrossRef](#)]
22. Zhou, H.; Chen, Y. Effect of acidic surface functional groups on Cr(VI) removal by activated carbon from aqueous solution. *Rare Met.* **2010**, *29*, 333–338. [[CrossRef](#)]
23. Mamo, S.K.; Elle, M.; Baron, M.G.; Simons, A.M.; Gonzalez, J.R. Leaching kinetics, separation, and recovery of rhenium and component metals from CMSX-4 superalloys using hydrometallurgical processes. *Sep. Purif. Technol.* **2018**, *212*, 150–160. [[CrossRef](#)]
24. Yang, J.H.; He, L.H.; Liu, X.H.; Ding, W.T.; Song, Y.F.; Zhao, Z.W. Comparative kinetic analysis of conventional and ultrasound-assisted leaching of scheelite by sodium carbonate. *Trans. Nonferrous Met. Soc. China* **2018**, *28*, 775–782. [[CrossRef](#)]
25. Li, L.; Zhai, L.Y.; Zhang, X.X.; Lu, J.; Chen, R.J.; Wu, F.; Amine, K. Recovery of valuable metals from spent lithium-ion batteries by ultrasonic-assisted leaching process. *J. Power Sources* **2014**, *262*, 380–385. [[CrossRef](#)]
26. Diehi, O.L.; Gatiboni, T.L.; Mello, P.A.; Muller, E.I.; Duarte, F.A.; Loes, E.M.M. Ultrasound-assisted extraction of rare and precious-earth elements from carbonatite rocks. *Ultrason. Sonochem.* **2018**, *40*, 24–29.
27. Zhang, D.L.; Li, M.; Gao, K.; Li, J.F.; Yan, Y.J.; Liu, X.Y. The physical and chemical mechanism underlying ultrasonically enhanced hydrochloric acid leaching of non-oxidative roasting of bastnaesite. *Ultrason. Sonochem.* **2017**, *39*, 744–781. [[CrossRef](#)] [[PubMed](#)]
28. Kong, J.; Xing, P.F.; Wei, D.H.; Jin, X.; Zhuang, Y.X. Ultrasound-assisted leaching of iron from silicon diamond-wire saw cutting waste. *JOM* **2021**, *73*, 791–800. [[CrossRef](#)]
29. Santos, E.V.D.; Saez, C.; Caizares, P.; Martinez-huitle, C.A.; Rodrigo, M.A. Treating soil-washing fluids polluted with oxyfluorfen by sono-electrolysis with diamond anodes. *Ultrason. Sonochem.* **2017**, *34*, 115–122. [[CrossRef](#)]
30. Hua, I.; Hoffmann, M.R. Optimization of ultrasonic irradiation as an advanced oxidation technology. *Environ. Sci. Technol.* **1997**, *31*, 2237–2243. [[CrossRef](#)]